AE-287
UDC 539.144.6

AE-287

Absolute EI, $\Delta K = O$ Transition Rates in Odd-Mass Pm and Eu-Isotopes

S. G. Malmskog

AKTIEBOLAGET ATOMENERGI
STOCKHOLM, SWEDEN 1967

ABSOLUTE E1, ΔK = 0 TRANSITION RATES IN ODD-MASS Pm and Eu-ISOTOPES

Sven G. Malmskog

ABSTRACT

The half life of the $5/2^-(532)$ intrinsic state in ^{151}Pm, ^{153}Eu and ^{155}Eu has been determined by the delayed coincidence method. The absolute E1, $\Delta K = 0$ transition probabilities between the $5/2^-$ $(532) \rightarrow 5/2^+(413)$ intrinsic states have been deduced and compared with theoretical predictions, using the Nilsson model as a starting point. The effect on the predicted transition probabilities obtained by adding pairing correlations and Coriolis coupling have also been studied. It has been found that the experimental transition rates, which are still strongly enhanced, cannot be explained by these contributions alone. It is therefore suggested that collective dipole contributions like those arising through the octupole excitations are of importance.

Printed and distributed in July 1967.

LIST OF CONTENTS

1. INTRODUCTION

It has been known for some time [e.g. ref. 1] that the experimentally observed E1 transition rates are considerably lower than expected from the single particle estimate [2]. In the deformed mass regions this is partly understood within the Nilsson model [3] from the fact that the main E1 strength is connected with the undisturbed oscillator excitations with energies of several MeV and thus, according to the E1 sum rule, very little of the E1 strength is left for the disturbed low lying excitations. This usually means that the E1 transitions can only take place via some small amplitude components in the wave functions and, furthermore, these terms do often add destructively. Vergnes [4] divided the E1 transitions into two groups, one with $\Delta K = 0$ where agreement with the Nilsson model was obtained and another with $|\Delta K| = 1$ where the transition rates were slower than expected from this model. By the addition of new experimental data [5], however, this boundary now tends to be smeared out.

The inclusion of the pairing correlations has been shown to have a drastic effect on the E1 transition rates [6, 7]. In many cases the predicted E1 transition rates are lowered by as much as two to three orders of magnitude as compared with the pure Nilsson model. Each case has, however, to be studied separately as the magnitude of the pairing reduction factor is critically dependent on the position of the single-particle orbitals pertinent to the initial and final excitations relative to the Fermi surface. As a general result of the inclusion of pairing correlations the overall agreement with theory for $|\Delta K| = 1$ transition rates is better, while the $\Delta K = 0$ transition rates are generally enhanced by two to three orders of magnitude.

Very few detailed calculations investigating the influence of the Coriolis coupling on the E1 transition rates have been performed. We know, however, that Coriolis mixing is of vital importance in explaining certain E1 transition rates like those of the K-forbidden type. It is thus possible that important effects also may be obtained in calculating the K-allowed transition rates.

Recently it has been suggested [8, 9, 10] that the collective contributions to the E1 transition rate obtained due to particle-vibration interaction with the octupole vibrational bands may be responsible for the enhanced transition rates observed.

In this work we have studied the $5/2^-(532) \rightarrow 5/2^+(413)$ transition rates in ^{151}Pm, ^{153}Eu, ^{155}Eu and ^{161}Tb. Section 3 describes the measurement of the half life of the $5/2^-(532)$ intrinsic particle state in the first three of these nuclei. Subsections 4.1 - 4.4 contain a quantitative discussion within the framework of the Nilsson model [3] including pairing correlations and Coriolis coupling. Finally in subsection 4.5 some general arguments regarding the quasi-particle interaction are given and the importance of adding E1 contributions from excitations of essentially octupole character is pointed out.

2. EXPERIMENTAL TECHNIQUE

The half life measurements to be described in this paper have all been performed using the delayed coincidence method. The instrumental set up includes a long lens electron-electron coincidence spectrometer very similar to the one described by Gerholm and Lindskog [11], a time-to-pulse height converter and a multichannel analyser. The spectrometer is equipped with a specially insulated source holder which makes it possible to apply a high tension of 20 kV to the source. A vacuum lock makes it possible to change the active sources in less than 30 seconds without breaking the high vacuum in the spectrometer. This is a facility that is necessary when working with short lived activities.

The electron detector in each spectrometer consists of a conical Naton 136 plastic scintillator cemented to a specially shaped light guide [12], which was optically coupled to the 56 AVP photomultiplier. In some of the measurements one lens was replaced by a 56 AVP photomultiplier furnished with a 25 mm x 25 mm cylindrical Naton 136 plastic scintillator placed 8 mm from the active source. If possible we preferred such a system to the electron-electron set up because of its higher efficiency and the convenience of using ^{60}Co as a prompt comparison source. The time resolution of the total electronic system in the latter set up was 450 psec as measured from a prompt $\beta \rightarrow \gamma$ coincidence curve with a ^{60}Co source. The linearity, stability and time calibration of the time-to-pulse height converter were checked several times during the actual measurements using an air core delay line similar to the one described by Graham et al. [13]. Due to the influence from the small insulating rods used to support the conducting copper wire, the velocity of the relevant timing pulses is smaller in this delay line than it would be in dry air. The absolute value of the time delay caused by the delay line was therefore checked against the velocity of light following the method given previously [14]. It was then found that a correction of 0.7 per cent should be applied to take into account the influence from the surrounding insulating material.

3. HALF LIFE MEASUREMENTS AND RESULTS

3.1 The 116.9 keV level in ^{151}Pm

Neodymium oxide enriched to 95.7 per cent in ^{150}Nd was mixed with pure alcohol and the resulting suspension was centrifuged onto thin backings of VYNS on which a thin layer of gold had been evaporated. Several sources with a thickness between 0.2 and 0.5 mg/cm^2 and with 3 mm diameter were prepared in this way. By irradiating these sources for some minutes in the R2-0 reactor at Studsvik with a thermal neutron flux of 10^{13} n/cm^{2}sec, active sources of the 12 min ^{151}Nd isotope were produced. These sources were only re-activated a few times in order to diminish the building up of the natural background from the daughter activity ^{151}Pm ($T_{1/2}$ = 28 hours).

The 116.9 keV level is strongly fed by gamma rays with energies of 737, 798 and 1180 keV, while no β branch to this level has been found [15,16]. A delayed coincidence measurement utilising the mentioned gamma rays detected in the 25 mm x 25 mm Naton 136 plastic scintillator furnished with a 5 mm Al-absorber and the 116.9 K conversion line was performed. The prompt (<2 psec) $\beta \rightarrow \gamma$ cascades in ^{60}Co were used to obtain a reference time distribution. These two types of measurements were registered in pairs using constant energy settings. A set of such a pair of curves is shown in fig. 1. The small tail on the right-hand side of the $\gamma \rightarrow$ 116.9 K decay curve originates from $\gamma \rightarrow$ 80.3 L and partly also from brems-strahlung $\rightarrow$ 80.3 L coincidences introducing the 0.9 nsec half life of the 255.7 keV level. The influence from this tail was experimentally taken care of by only shifting the electron channel to the 138.8 K line and measuring the decay curve caused by the 255.7 keV level. A normalised part of this curve was then subtracted from each of the $\gamma \rightarrow$ 116.9 K time distributions. A special correction to the measured time shift from a possible low energy tail of the 85.0 L conversion electrons is not necessary as these electrons are preceded by a 170.8 keV from the 255.7 keV level and thus taken care of by the subtraction procedure described above. The remaining curve, together with a prompt ^{60}Co curve, were analysed according to the centroid shift method [17]. As an average value from the analysis of several sets of time distributions we obtain a half life of $T_{1/2}$ = 89 ± 15 psec for the 116.9 keV level in ^{151}Pm. This is in agreement with the upper limit of $T_{1/2} \leq$ 300 psec given by Fossan et al. [18].

From the K-conversion coefficient and the K/L-ratio Blinowska et al. [16] found the 116.9 keV transition to have an E1 multipolarity and is thus expected to proceed between members of rotational bands belonging to different intrinsic states. The spin of the ground state in ^{151}Pm has been measured to 5/2 using the atomic beam magnetic resonance method [19] but the parity of this level is not known. According to some recent calculations by S.G. Nilsson et al. [20] the 61st proton is expected to be in the $5/2^+(413)$ orbit for a deformation $\delta < 0.25$ and in the $5/2^-(532)$ orbit for $\delta > 0.25$. The deformation of the ^{151}Pm nucleus can be determined from the measured spectroscopic quadrupole moment Q = 1.9 ± 0.3 barns [21] using the following expression obtained in the strong coupling scheme [22].

$$Q = \frac{4}{5} Z R_z^2 \, \delta \, (1 + 0.5 \, \delta) \times \frac{3K^2 - I(I+1)}{(I+1)(2I+3)} \qquad (1)$$

Inserting the values Q = 1.9 ± 0.3 barns, I = K = 5/2, R_z = 1.2 fm and Z = 61 we obtain δ = 0.23 ± 0.03. This deformation indicates positive parity for the ground state but is by no means a strong argument. The magnetic moment of the ground state in ^{151}Pm is measured to μ = 1.8 ± 0.2 n.m. [21]. In fig. 2 the theoretical predictions of μ from the Nilsson model for the two K = 5/2 orbitals, $5/2^+(413)$ and $5/2^-(532)$, are compared with the experimental value. In the calculation, effective values of the gyromagnetic factor g_s have been used. Agreement is obtained for the $5/2^+(413)$ orbital when the rather low value of $g_s eff <$ 0.6 g_s is used. Unfortunately, when Coriolis mixing is taken into account, the admixture from the $3/2^-(541)$ orbital, has a tendency to decrease the predicted value of the magnetic moment for the $5/2^-$ (532) level, while the predicted value of μ for the $5/2^+(413)$ level seems to be quite insensitive to possible Coriolis admixtures. This will of course make the choice of ground state orbital from the measured magnetic moment more delicate especially as uncertainties in the nuclear model itself also has to be taken into account. Throughout the following work we have regarded $5/2^+(413)$ as the ground state orbital in ^{151}Pm. We will, however, point out that in the discussion to follow, all the essential conclusions will still be valid with a $5/2^-(532)$ orbital assignment for the ground state in ^{151}Pm.

From table 1 it is seen that the 116.9 keV E1 transition has the unusually low F_W-value of 650. In the deformed region such low values of F_W have only been observed for E1 transitions with $\Delta K = 0$ [5]. It is thus very tempting to suggest that the 116.9 keV E1 transition takes place between levels with the same K-quantum number. The only reasonable assignment to the 116.9 keV level is then $5/2^-(532)$ which is actually expected to be a low energy level in the Pm isotopes [22].

3.2 The 97.4 keV level in ^{153}Eu

The 97.4 keV level in ^{153}Eu is strongly fed by an electron capture branch in the decay of the 242 days ^{153}Gd activity. The de-excitation of this level mainly takes place by a 97.4 keV E1 transition.

Active ^{153}Gd in a HCl solution was bought from Amersham with a specific activity of 1 mc ^{153}Gd/g Gd. Thin electron sources were prepared by evaporating a small droplet on a backing of VYNS on which a thin layer of gold had been vacuum evaporated.

The relevant part of an electron spectrum obtained with such a source placed in the lens spectrometer is shown in the right-hand part of fig. 3. As is seen from this figure the 103.2 K and 97.4 K electron lines together with the Auger electron group form a complex of lines where the individual components are only partly resolved from each other.

One lens was adjusted to focus the 97.4 K line while the other lens accepted KLL Auger electrons. Due to limited resolution of the spectrometer and the finite thickness of the source, coincidences from the 103.2 K tail → KLL Auger electron cascade were also accepted. Fig. 3 shows a representative delayed coincidence curve measured during a 24 hours run with the energy settings given above.

The slow decay component on the righ-hand side is caused by the 3.7 nsec half life of the 103.2 keV level in ^{153}Eu. The lifetime of the 97.4 keV level was obtained in the following way. The 97.4 K → KLL Auger coincidence time spectrum was registered in periods of 60 minutes. Between these periods other 60 minute measurements were performed on the 94.7 K → β^- cascade obtained in the decay of the 2.4 hours ^{165}Dy isotope which we used to define a reference time. The intermediate 94.7 keV level in ^{165}Ho is known to have a mean life of 26 psec [23]. In order to be able to keep the same energy settings in the two types of measurements we accelerated the 94.7 K electrons by applying a 10 kV negative high tension to the ^{165}Dy source. To properly correct for the influence from the 3.7 nsec decay component this was also measured in a separate run using the 103.2 K → KLL Auger electron cascade. The resulting decay curve was then normalized and subtracted from each 97.4 K → KLL Auger curve before the final analysis was performed.

All the experimental data were analysed according to the centroid shift method [17]. After correction for the mean life of the 94.7 keV level in ^{165}Ho and the small shift introduced in the acceleration procedure we obtain a half life of $T_{1/2}$ = 180 ± 20 psec for the 97.4 keV level in ^{153}Eu.

The half life of this level has been determined before using nuclear resonance scattering methods. The results from earlier measurements as well as our new value are shown in table 2.

3.3 The 105 keV level in ^{155}Eu

The 105 keV level in ^{155}Eu is very strongly populated by β particles (93 %) in the decay of the 22 min ^{155}Sm isotope. The feeding of gamma rays to this level is roughly 2 % [24]. The ^{155}Sm-activity used in this work was produced by neutron irradiation of samarium-oxide enriched to 99.2 % in ^{154}Sm. The active electron sources were prepared following the same procedure as described in section 3.1. For the delayed coincidence measurements to be described we made use of the feeding β particles and the K conversion electrons from the 105 keV transition.

In the first type of experiment the 105 K line was focussed in one lens while the β continuum with an energy larger than 600 keV was detected in a 25 mm x 25 mm Naton 136 plastic scintillator placed 3 mm from the source. Several delayed time distributions were recorded with these energy settings for about half an hour each time. In between these measurements were sandwiched corresponding runs in which the Sm source was substituted by a ^{60}Co source without any changes in the energy settings. The time delay in ^{60}Co between the β continuum measured in the lens spectrometer and the high energy gamma rays measured in the plastic scintillator is negligible (<2 psec). These pairs of time distributions were analysed using the centroid shift method [17] from which, as an average result, a half life of 90 ± 15 psec was deduced for the 105 keV level in ^{155}Eu.

In a second type of experiment both electron lenses were used, and a self comparison measurement of the type proposed by Bell et al. [25] was performed. To reduce the systematic errors introduced when the conversion electron lines are shifted between the two lenses we used fixed energy settings and instead altered the electron energy by means of an electrostatic high tension applied to the source as described by Lindskog and Sundström [26]. The first lens was thus focussed on the 105 K conversion electron line (57 keV) while the second lens was focussed on the β continuum at an energy of 67 keV (see fig. 4). With these energy settings we essentially measured the delayed time distribution between the 105 K and the directly feeding β-particles. Then we applied so much negative high tension to the source that the 105 K line was focussed in the second lens. The first lens then became focussed on the β-continuum below the 105 K line (see fig. 4). Several time shifts between delayed coincidence curves obtained with and without high tension were recorded. A typical example of such a pair of curves is given in fig. 4. The average measured centroid shift obtained from several such pairs of curves is 288 ± 18 psec, which roughly corresponds to twice the mean life of the 105 keV level [25].

Some corrections to this value, however, have to be considered in the present case. Two per cent of the 105 K electrons are fed by β-particles via higher excited levels in ^{155}Eu [24]. The main part of these electrons (80 %) are fed by the 141 transition de-exciting the 246 keV level with a measured half life of 1.38 nsec [27]. The small influence from these extra delayed 105 K electrons on the centroid shift of the measured time distribution has been taken into account in the analysis of the data. The remainder of these special 105 K electrons (20 %) are fed from levels whose half lives are approximately equal to or less than that of the 105 keV level. The extra shift obtained from these electrons can be disregarded. The possible contribution of β-79 L-tail coincidences to the decay curve measured without high tension was determined by taking coincidences between the 79 L-tail and the β-continuum at 180 keV where no conversion lines are found. The undesirable coincidence contribution involving the 79 L line was in this way determined to be less than two per cent of the coincidence counting rate involving the 105 K peak. The influence from the coincidences involving the 61 L - β cascade is difficult to measure as the 61 L line is completely masked by the strong 105 K line. An estimate of its influence can, however, be obtained. From the gamma ray intensity ratio 105 keV/61 keV = 445 [24] and the theoretical conversion coefficients [28] the electron intensity ratio 105 K/61 L is given as 87. Furthermore the 307 keV level, which is the first excited rotational level built on the 246 keV $3/2^+(411)$ ground state, is mainly de-excited by this 61 keV transition. It is well known that the absolute M1 strength for such an interband transition is well described by the Nilsson model if an effective value of the gyromagnetic factor g_s is used [29]. The partial M1 half life for the 61 keV transition is then obtained from

$$T_{1/2\gamma}(M1) = \frac{27.7 \times 10^{-5}}{E_\gamma^3(1+\alpha)(1+\delta^2)(g_K - g_R)^2} \qquad (2)$$

where E_γ is the transition energy in keV. For a deformation of $\eta = 5$ and an effective g_s-value of 70 per cent of the free proton value (g_s free = 5.585) the parameter g_K is deduced to be 1.7. A reasonable value of g_R is 0.4. Using these two values together with $E_\gamma = 61$ keV, $\alpha(M1) = 10$ and $\delta = 0$ we obtain $T_{1/2} = 65$ psec. When the necessary corrections are made for other weaker transitions leaving the 307 keV level its half life is estimated to $T_{1/2} = 63$ psec. Even if this estimate is wrong by as much as a factor of two, the total additional shift to the measured $\beta \rightarrow 105$ K decay curves from the $\beta \rightarrow 61$ L cascade will be less than 2 psec, mainly because of the low intensity of the 61 L line and the approximately equal half lives of the 105 and 307 keV levels.

When the decay curve with high tension is measured, the first lens is focussed on the β-continuum below the 105 K line. Because of the thickness of the active curve some 105 K electrons will lose enough energy to enter into the first lens and unwanted coincidence between 105 K - β will be registered. The time distribution from such cascades will have a time shift equal in magnitude but with opposite direction to the main contribution of β - 105 K coincidences. From the intensity ratio shown on the right-hand side of fig. 4 the time shift in this latter case will be $(0.86 \pm 0.04)\ \tau$ instead of τ which it should have been if the influence from the tail of the 105 K line could be disregarded. Finally the influence from the finite acceleration distance has been estimated to < 2 psec. When these corrections have been taken into account a half life of 107 ± 10 psec is obtained. The weighted average value from the two different types of measurements reported here is $T_{1/2} = 104 \pm 10$ psec, which is also taken as the half life of the 105 keV level in ^{155}Eu. This result is in agreement with the upper limits of < 400 psec [30] and < 200 psec [27] given earlier for this half life.

4. DISCUSSION

4.1 Survey of the relevant data

All the pertinent data regarding the E1 transitions between the $5/2^-$(532) and $5/2^+$(413) orbitals in ^{151}Pm, ^{153}Eu, ^{155}Eu and ^{161}Tb have been compiled in table 1. From the measured half lives, gamma ray and conversion electron intensities, the partial gamma ray half lives ($T_{1/2\gamma}$) have been deduced. This table also gives the hindrance factors calculated relative to the single-particle Weisskopf estimate

$$F_W = T_{1/2\gamma}\,(\text{exp})/T_{1/2\gamma}(\text{Weisskopf})$$

and relative to the Nilsson model

$$F_N = T_{1/2\gamma}(exp)/T_{1/2\gamma}(Nilsson)$$

To obtain the Weisskopf estimate a nuclear radius of 1.2 fm and a statistical factor equal to one was used [2]. In the calculation of the Nilsson unit the amplitudes of the eigen-functions were chosen in accordance with ref. [3]. The value "f" given in table 2, column 11 gives a rough estimate of the limits for the hindrance factors F_W and F_N. These limits are obtained by multiplying and dividing the given F-values by "f". A more detailed discussion of the experimental results in the light of the Nilsson model, with the inclusion of pairing correlations, Coriolis coupling and octupole vibrations, is given in the following subsections.

4.2 Nilsson model

A simple model with which to compare the experimentally observed E1 transition rates is that obtained by regarding a single particle moving in the deformed potential created by the other particles. Such a model has been described in detail by Nilsson [3]. The wave functions in that work are given as a sum of eigen-functions of the isotropic harmonic oscillator. The amplitudes of these eigen-functions depend on the deformation δ and on the two potential parameters, κ and μ, which were determined from a comparison with the experimentally known level systematics in 1955 [3]. To find out whether the values of κ and μ adopted from that work are still representative in the present mass region, a semiempirical level scheme has been determined so that a BCS blocking calculation with G = 0.16 MeV and including 30 levels [31], roughly reproduces the presently known energies of the intrinsic states. The single-particle states needed in this calculation are given in fig. 5, together with levels calculated from the Nilsson model with δ = 0.3 and with the following potential parameters:

$$\kappa = 0.06,\ \mu = 0.55 \text{ for } N = 4 \text{ and } \kappa = 0.06,\ \mu = 0.45 \text{ for } N = 5.$$

These values are close to the set of parameters recommended by Nilsson [3]. Several other sets of δ, κ and μ were also investigated in a systematical way, but no one gave a better agreeement between the Nilsson levels and the calculated semiempirical levels (e.g. it was the only set of $\varkappa$ and μ parameters which gave the correct level order). The wave functions obtained from the above $\varkappa$ and μ parameters are therefore used for the further calculations of the quantities G_{E1} (defined in ref. [3]) and the Coriolis matrix elements $\langle IK|j_{\pm}|I'K'\rangle$ [32]. These values are presented in the upper part of table 3. It should be pointed out that, although the energy level order changed for the different choices of the parameters δ, $\varkappa$ and μ, all the relevant quantities as G_{E1} and $\langle IK|j_{\pm}|I'K'\rangle$ only showed minor variations (< 20 %). Because of this relative stability of the predicted quantities, we assume that these can be used for the quantitative estimates to follow below, although all the G_{E1}-values as well as the $\langle 5/2^+(413)|j_+|3/2^+(411)\rangle$ Coriolis matrix element are asymptotically forbidden.

According to the Nilsson model the partial gamma ray E1 transition probability is given by the following expression.

$$T_{1/2\gamma}(E1) = \frac{1.81 \times 10^{-15}}{A^{1/3}(1-\frac{Z}{A})^2 E_\gamma^3} \times \tag{3}$$

$$\times \frac{1}{|\langle IK1, K'-K|I'K'\rangle + b_{E1}(-1)^{I'+K'}\langle IK1,-K'-K|I',-K'\rangle|^2 G_{E1}^2}$$

where E_γ is the transition energy in MeV and $T_{1/2\gamma}$ is given in sec. The comparison with experiment is generally made by giving the hindrance factor F_N. The numerical values of this factor for the nuclei studied in this work are given in table 1, column 10 and also plotted in the left-hand part of fig. 6. The uncertainty limits given are only those from the experiments. It is seen from fig. 6 that all these E1 transitions are enhanced by approximately a factor of 50 as compared with the Nilsson model values. This is an unusual behaviour since almost all E1 transition rates in the deformed mass regions are either equal to, or hindered as compared to the Nilsson estimate [5]. The possible reasons for this enhancement must be further investigated.

4.3 Influence of pairing correlations

The inclusion of pairing correlations has the effect of giving a diffuse Fermi surface which introduces a change in the transition matrix element between single-particle states but does not influence the relative behaviour of the E1 transition rates from the 5/2 $5/2^-$ state to the different levels in the $5/2^+$ band. The hindrance factor for the E1 transitions defined in the quasi-particle model taking pairing into consideration can be written

$$F_{QM} = P_-^2 F_N \quad \text{where } P_\pm \approx (UU' \pm VV')R \qquad (4)$$

In this approximation the factors U and V give the probability amplitude that the level in question is unoccupied or occupied, respectively, by a pair of particles. R is a factor close to one. From the fact that the pairing factors are always equal to or less than one, eq. (4) immediately gives that the inclusion of pairing correlations will in this case further deteriorate the possibilities to get agreement with experiment. For the discussion to come in subsections 4.4 and 4.5, however, it is of interest to have a quantitative figure on the influence of pairing correlations on the transition probabilities. We have therefore carried through a numerical calculation.

The pairing factors $P_\pm$ used in this work are obtained from the BCS blocking calculations using the semiempirical energy levels given in fig. 5. The numerical values of P_- and P_+ are presented in table 3. The uncertainties given are those of the BCS approximation itself [33] as well as from the single-particle levels. The errors of the latter kind have been estimated by varying the parameters of the deformed potential and seem to give an accuracy better than ± 20 %. All the $|P_-|$ values are seen to be well below one and will thus make the experimental E1, $\Delta K = 0$ transitions still more enhanced relative to the quasi-particle model estimate. The effect is especially large in the case of ^{153}Eu where the predicted $5/2^-(532) \to 5/2^+(413)$ transition rate is decreased by more than one order of magnitude. The result is displayed in the middle part of fig. 6, where the given limits are those from theoretical estimates. From this figure it is seen that, to obtain agreement with experiment, we are forced to include other terms in our theoretical estimates like the one coming from non-adiabatic effects and/or interactions between quasi-particles.

4.4 Influence of Coriolis admixtures

For low-lying energy states the most important non-adiabatic effect consists in the Coriolis coupling of levels with $|\Delta K| = 1$ or $K = K' = 1/2$. In the present case the strongest admixtures to the $5/2^+(413)$ and $5/2^-(532)$ bands are expected to come from the $3/2^+(411)$, $3/2^+(422)$ and the $3/2^-(541)$ orbitals which are rather close in energy. The reduced E1 transition probability to first order (only terms involving at least one of the main components are included) is then given by

$$B[E1;\ 5/2\ 5/2^-(532) \rightarrow I\ 3/2^+(413)] = \frac{3}{4\pi} \cdot \frac{\hbar e^2}{M\omega_o} \left(1 - \frac{Z}{A}\right)^2 \times$$

$$\times \left| \sum_{K^-K^+} a_{K^-} a_{K^+} \langle 5/2\, K^- 1, K^+ - K^- | I K^+ \rangle G_{E1}(K^- \rightarrow K^+) \cdot P_-(K^- \rightarrow K^+) \right|^2 \tag{5}$$

The amplitudes a_{K^-} and a_{K^+} are, for the main components, equal to 1, while for the admixed components perturbation theory gives

$$a_K(I) = -\frac{\hbar^2}{2\mathcal{J}} \cdot \frac{P_+ \langle K | j_\pm | K' \rangle \sqrt{(I - 3/2)(I + 5/2)}}{E(I, 5/2) - E(I, 3/2)} \tag{6}$$

The denominator should be taken equal to the experimental level energy difference in keV if measured. Otherwise this quantity has to be estimated by the aid of the single-particle level scheme given in fig. 5 taking into account the compression of the band head energies as obtained from the BCS calculation. The quantities needed to calculate the reduced transition probability B(E1) are given in table 3. In evaluating the amplitudes of the admixtures (eq. 6) the factor $\hbar^2/2\mathcal{J}$ was chosen as 12 keV in all cases.

The Coriolis matrix elements for mixing the $3/2^-(541)$ and $3/2^+(422)$ orbitals into the main $5/2^-(532)$ and $5/2^+(413)$ components, respectively, are much larger than for the $3/2^+(411)$ orbital (table 3). As this is roughly compensated for by the variation in the energy difference $E(I, 5/2) - E(I, 3/2)$, all the admixed amplitudes are of the same order of magnitude $[0.04 \leq |a_K(I)| \leq 0.16]$. Furthermore it turns out that the Coriolis contributions to the transition rates in all cases except ^{151}Pm are destructive. The E1, $\Delta K = 0$ transition rates in ^{153}Eu are the ones most sensitive to admixtures, since the contribution of the main $5/2^-(532) \rightarrow 3/2^+(413)$ component in this case is strongly reduced by the P_- pairing factor. The resulting retardation factor, F_{PC}, taking pairing correlations and Coriolis coupling into account, is presented in the right-hand part of fig. 6 together with the upper and lower limits from the theoretical predictions. The influence from the Coriolis coupling on the E1 transition rates is in all cases limited to less than a factor of 2 and can thus by no means offer an explanation of the observed enhanced E1, $\Delta K = 0$ transition rates.

4.5 Quasi-particle interaction

As argued in the previous discussion, the contribution to the E1 transition rates obtained from the Nilsson model with the inclusion of pairing correlations and Coriolis admixture do not seem large enough to explain the experimental transition rates, being a factor of a hundred to a thousand larger than given by the results of these estimates. We thus seem forced to include effects of interactions between quasiparticles. In particular we have to consider the particle-vibration interaction. Of the relevant vibrational modes, the electric dipole excitation has a high energy (> 10 MeV) while both quadrupole and octupole vibrational modes are found with energies less than 2 MeV. These are therefore expected to give comparatively larger perturbations to the low-lying energy levels of present interest. From recent calculations, Soloviev and Vogel [34] have made predictions indicating that low-lying energy states in deformed odd-mass nuclei roughly consist, to 95 per cent, of the proper Nilsson orbital, while the remaining 5 per cent is shared between quadrupole and octupole admixtures. The quadrupole admixtures can only give rise to a slight renormalization of the E1 transition rates. The octupole vibrational coupling, on the other hand, will mix the octupole levels built on the final $5/2^+$ intrinsic state into the initial $5/2^-$ intrinsic state and vice versa.

In even deformed nuclei the lowest octupole excitations will have $K^\pi = 0^-, 1^-, 2^-$ and 3^-. Of these only the 0^- and 1^- levels seem to have been experimentally observed in the mass region at $A \sim 150$. These two octupole vibrational bands will both be mixed with the main Nilsson components. As their mixing amplitudes are in both cases proportional to matrix elements of a one-body operator, the same pairing factor P_- as for the main orbitals should be used. The calculated E1 transition rates will therefore still be proportional to P_-^2 and the effect of the pairing correlations as discussed above will remain.

To introduce some qualitative arguments about the influence from the octupole vibrations we can write the quasi-particle state wave function in a semiclassical one-phonon approach as

$$|K^{\pi};0,0;K^{\pi},I\rangle + \sum_{K' K_{\omega} K_t} C_{\omega}(K',K_{\omega},K_t)\,|K'^{\pi'};1,K_{\omega};K_t^{\pi},I\rangle$$

In the state vector $|K'^{\pi'};\nu,K_{\omega};K_t^{\pi},I\rangle$, K_{ω} equals the component of the phonon angular momentum along the nuclear symmetry axis and $K_t = |K \pm K_{\omega}|$. Furthermore the relations $\pi\pi' = (-1)^{\nu}$ and $I \geq K_t$ will hold. The discussion is limited to the angular momentum components $K_{\omega}^{\pi} = 0^-$ and 1^-, which will both be responsible for the octupole admixtures. In evaluating the E1 transition rates only such terms, besides the single-particle contribution, which incorporate a collective E1 strength (transitions with $|\Delta\nu| = 1$) are considered. An estimate of this collective E1 octupole strength is obtained from the Coulomb excitation of the 0.96 MeV 1^- level in ^{152}Sm [35] which gives $B(E1;1^- \rightarrow 0^+) \sim 8 \times 10^{-3}\ e^2fm^2$. The value obtained from the Nilsson model for the relevant $B(E1;5/2^- \rightarrow 5/2^+)$ is $\sim 5 \times 10^{-5}\ e^2fm^2$. The E1 strength from the 0^- octupole admixtures may be even larger than for the 1^- component [9,10]. The effect on the E1 transition rate will be strongly dependent on the sign relations between the different components in the state wave function.

If we admit a 5 % octupole admixture as an upper limit into both the initial and final states and furthermore assume that all the components add coherently, we can obtain an octupole contribution to the E1 transition rate of between one and two orders of magnitude larger than the previously calculated single-particle contributions. This is sufficient to explain the enhancement found for the E1 transition rates in ^{151}Pm and ^{161}Tb. In the europium cases, however, the adopted E1 octupole strength, together with the upper limit of 5 % octupole admixture, does not seem to be sufficient to account for the observed enhancement.

In a recent calculation using a microscopic approach, Monsonego and Piepenbring [9] have demonstrated that, at least for the ^{153}Eu and ^{155}Eu nuclei, the octupole admixture gives the dominating contribution to the $\Delta K = 0$, E1 transition rate. They have also carried out the numerical calculation for two values of the octupole interaction strength parameter χ giving enhancements of 100 and 1000 respectively over the single-particle plus pairing estimate. This is in rough agreement with the crude estimates above. Unfortunately we do not know the value of χ which corresponds to a realistic octupole E1 strength, e.g. as the one determined from the 0.96 MeV level in ^{152}Sm [35].

It is also interesting to note that according to Mottelson and Nilsson [36] the deformation of the $5/2^-(532)$ orbit in ^{153}Eu may be significantly lower than for the $3/2^+(413)$ orbit. It has been demonstrated earlier [27] that the effect of a 10 % change in the deformation in this case will increase the $5/2^-(532) \rightarrow 5/2^+(413)$ E1 transition rate by roughly an order of magnitude. Such a contribution will help in understanding the observed enhancement.

In conclusion, we have found that the quasi-particle model including Coriolis coupling is by no means capable of accounting for the main features of the $\Delta K = 0$, E1 transition rates in the presently studied nuclei. We also find that the octupole contributions together with effects from possible deformation changes may well be sufficient to explain the observed enhancement for these transitions.

The author is indepted to Drs. Anders Bäcklin and Sven Wahlborn for valuable criticism of the present work.

Table 1

Pertinent information on the $5/2^-(532) \rightarrow 5/2^+(413)$ E1 transitions in ^{151}Pm, ^{153}Eu, ^{155}Eu and ^{161}Tb.

Nucleus	$T_{1/2}$(exp) of level in psec	Transition energy in keV	Initial state I $K^{\pi}[Nn_z\Lambda]$	final state I $K^{\pi}[Nn_z\Lambda]$	Relative N_{γ} a)	Relative N_e a)	$T_{1/2\gamma}$(exp) in sec	F_W b)	F_N c)	f d)	η e)	References
^{151}Pm	89±15	116.9	5/2 $5/2^-(532)$	5/2 $5/2^+(413)$	340	59	10.4×10^{-11}	700	2.4×10^{-2}	1.3	4	$T_{1/2}$: f) $N_{\gamma}N_e$: g)
^{153}Eu	180±20	97.4	5/2 $5/2^-(532)$	5/2 $5/2^+(413)$	3000	890	2.4×10^{-10}	930	3.1×10^{-2}	1.3	5	$T_{1/2}$: f)
		14.0		7/2 $5/2^+(413)$	2.1	10	3.3×10^{-7}	4.0×10^{3}	5.3×10^{-2}	2.5		$N_{\gamma}N_e$: h) i)
^{155}Eu	104±10	105	5/2 $5/2^-(532)$	5/2 $5/2^+(413)$	200	48	1.3×10^{-10}	650	2.2×10^{-2}	1.3	5	$T_{1/2}$: f)
		26		7/2 $5/2^+(413)$	1.1	2.6	2.3×10^{-8}	1.7×10^{3}	2.4×10^{-2}	2.0		$N_{\gamma}N_e$: k)
^{161}Tb	<100	482	5/2 $5/2^-(532)$	3/2 $3/2^+(411)$	46	< 0.1	$<2.0\times10^{-10}$	$<1.0\times10^{5}$	<2.7		5	$T_{1/2}$: l)
		424		5/2 $3/2^+(411)$	3	< 0.1	$<3.1\times10^{-9}$	$<1.0\times10^{6}$	<12			$N_{\gamma}N_e$: m)
		165.3		5/2 $5/2^+(413)$	39	4.3	$<2.4\times10^{-10}$	$<4.8\times10^{3}$	<0.16			

a) N_{γ} and N_e are normalised for each nucleus such that, for each multipole transition, N_e/N_{γ} gives the total conversion coefficient.

b) Single particle estimate taken from ref. [2] using a statistical factor equal to one.

c) The calculated value of G_{E1} (from eq. (35b) in ref. [3]) increases only 5 % between η = 4 and η = 6.

d) Defined in the text of Section 4.1.

e) Deformation parameter according to the notation of Nilsson [3].

f) Present work. g) Ref. [16]. h) Ref. [23]. i) Ref. [28]. k) Ref. [24]. l) Ref. [8]. m) Ref. [40].

Table 2

Experimental results from the measurements of the half life of the 97.4 keV level in ^{153}Eu.

Method	Result $T_{1/2}$ in 10^{-12} sec.	Ref.
Regular nuclear resonance scattering	158 ± 21	[a]
Recoil less nuclear resonance scattering	214 ± 21	[b]
Delayed coincidence measurement using KX-rays → 97.4γ	≤ 350	[c]
Delayed coincidence measurement using KLL-Auger electrons → 97.4K electrons	180 ± 20	[d]

a) Ref. [37]
b) Ref. [38]
c) Ref. [39]
d) Present work

Table 3

Single-particle and Coriolis coupling matrix elements together with pairing factors for the Nilsson orbitals of interest in the present work.

	$5/2^-(532) \rightarrow 5/2^+(413)$ $G_{E1} = 0.014$	$5/2^-(532) \rightarrow 3/2^+(411)$ $G_{E1} = 0.013$	$5/2^-(532) \rightarrow 3/2^+(422)$ $G_{E1} = -0.042$	$3/2^-(541) \rightarrow 5/2^+(413)$ $G_{E1} = 0.0052$
	P_-	P_-	P_-	P_-
^{151}Pm	$+0.60 \pm 0.10$	$+0.8 \pm 0.2$	-0.27 ± 0.10	-0.45 ± 0.10
^{153}Eu	-0.25 ± 0.05	$+0.02 \pm 0.03$	-0.8 ± 0.2	-0.60 ± 0.10
^{155}Eu	-0.50 ± 0.10	$+0.10 \pm 0.10$	-0.8 ± 0.2	-0.70 ± 0.10
^{161}Tb	-0.85 ± 0.08	-0.7 ± 0.2	-0.9 ± 0.1	-0.85 ± 0.10

	$5/2^-(532),\ 3/2^-(541)$ $\langle 5/2^- \vert j_+ \vert 3/2^- \rangle = 5.3$	$5/2^+(413),\ 3/2^+(411)$ $\langle 5/2^+ \vert j_+ \vert 3/2^+ \rangle = 0.67$	$5/2^+(413),\ 3/2^+(422)$ $\langle 5/2^+ \vert j_+ \vert 3/2^+ \rangle = 3.2$
	P_+	P_+	P_+
^{151}Pm	0.79 ± 0.02	0.94 ± 0.01	0.83 ± 0.02
^{153}Eu	0.96 ± 0.02	0.99 ± 0.01	0.84 ± 0.02
^{155}Eu	0.97 ± 0.02	0.94 ± 0.01	0.92 ± 0.02
^{161}Tb	0.99 ± 0.01	0.95 ± 0.01	0.96 ± 0.02

FIGURE CAPTIONS

Fig. 1 The delayed coincidence curve indicated by crosses is taken between gamma rays > 700 keV and the 116.9 K conversion electrons. The slow decay component on the right-hand side originates from γ-80.3 L and brems-strahlung - 80.3 L coincidences introducing the 0.9 nsec half life of the 255.7 keV level. The dotted prompt reference decay curve is obtained using a ^{60}Co source. From the analysis (see text) the half life of the 116.9 keV level in ^{151}Pm was found to be 89 ± 15 psec. The right-hand part of the figure shows a pertinent part of the electron spectrum from the decay of ^{151}Nd measured in one lens.

Fig. 2 Comparison between the measured magnetic moment μ = 1.8 ± 0.2 n.m. for the ground state of ^{151}Pm and the predictions of the Nilsson model for the $5/2^{+}$(413) and $5/2^{-}$(532) orbitals. The calculation has been performed for the deformations η = 2 and 4 and with different effective values of the gyromagnetic factor g_s. The value of g_R was chosen as 0.40 ± 0.05.

Fig. 3 The delayed coincidence curve indicated by dots is taken between the 97.4 K → KLL Auger electrons in the decay of ^{153}Gd. The slow decay component on the right-hand side originates from 103.2 K tail → KLL Auger electron coincidences introducing the 3.7 nsec half life of the 103.2 keV level. The reference decay curve indicated by crosses is taken between the 94.7 K electrons (accelerated by 10 kV) and the β^{-} continuum in the decay of ^{165}Dy using the same energy settings as in the ^{153}Gd measurement. From the analysis (see text) the half life of the 97.4 keV level in ^{153}Eu was found to be 180 ± 20 psec. The right-hand part of the figure shows a pertinent part of the electron spectrum from the decay of ^{153}Gd measured in one lens.

Fig. 4 The two delayed coincidence curves shown are the results from a self comparison measurement using the 105 K-electron line and the β^- continuum in the decay of ^{155}Sm. From the analysis (see text) the half life of the 105 keV level in ^{155}Eu was found to be 104 ± 10 psec. The right-hand part of the figure shows a pertinent part of the electron spectrum from the decay of ^{155}Sm measured in one lens.

Fig. 5 The single-particle level scheme in the neighbourhood of the Fermi level (ϵ_F). To the left are the Nilsson levels for protons calculated with $\delta = 0.3$ and the potential parameters $\varkappa = 0.06$, $\mu = 0.55$ for N = 4 and $\varkappa = 0.06$, $\mu = 0.45$ for N = 5. To the right are the semiempirical levels found here to be appropriate for the Pm, Eu and Tb isotopes. In the present calculation the level $\epsilon(3/2^+)$ is fixed at 5.27 (unit $\hbar\omega_o$) and the levels $\epsilon(5/2^-)$, $\epsilon(5/2^+)$, $\epsilon(7/2^-)$ and $\epsilon(1/2^+)$ are given the locations as shown in the diagram. The locations of the other levels used in the pairing calculation are as follows:

<u>below $5/2^-(532)$ or $5/2^+(413)$</u>: 4.41, 4.44, 4.47, 4.54, 4.68, 4.75, 4.79, 4.83, 4.88, 4.91, 4.95, 5.02, 5.04 and 5.07;

<u>above $1/2^+(411)$</u>: 5.44, 5.47, 5.63, 5.64, 5.68, 5.70, 5.90, 5.91, 5.92, 5.97 and 6.00.

Fig. 6 Retardation factors for the E1, $\Delta K = 0$ transitions in the relevant Pm, Eu and Tb isotopes. The factor F_N is calculated from the pure Nilsson model. In the quasi-particle value, F_{QM}, the pairing correlations are included. For F_{PC} also the Coriolis coupling effect has been added. In the case of F_N the experimental errors are indicated. In the cases of F_{QM} and F_{PC} the nominal value together with the estimated upper and lower limits according to the theoretical calculations are shown. Crosses are $5/2\ 5/2^- \rightarrow 5/2\ 5/2^+$ transitions and circles $5/2\ 5/2^- \rightarrow 7/2\ 5/2^+$ transitions.

REFERENCES

1. STROMINGER D and RASMUSSEN J O,
Concerning lifetimes of low energy E1 gamma transitions in odd mass spheroidal nuclei.
Nuclear Physics 3 (1957) 197.

2. WAPSTRA A H, NIJGH G J and VAN LIESHOUT R,
Nuclear Spectroscopy Tables, North Holland Publ. Co., Amsterdam, 1959.

3. NILSSON S G,
Binding states of individual nucleons in strongly deformed nuclei.
Mat.-Fys. Medd. Danske Vid. Selsk. 29 (1955) no 16.

4. VERGNES M N,
Mise en évidence de deux classes de transitions E1 dans les noyaux déformés des terres rares.
Nuclear Physics 39 (1962) 273.

5. LÖBNER K E G and MALMSKOG S G,
Systematics of absolute gamma-ray transition probabilities in deformed odd-mass nuclei.
Nuclear Physics 80 (1966) 505.

6. MONSONEGO G and PIEPENBRING R,
Calcul des effets des corrélations de paires sur les transitions E1 dans les noyaux de masse impaire de la région des terres rares.
Nuclear Physics 58 (1964) 593.

7. VERGNES M N and RASMUSSEN J O,
Influence of pairing correlations on E1 transition probabilities in odd-mass deformed, rare-earth nuclei.
Nuclear Physics 62 (1965) 233.

8. MALMSKOG S G, MARELIUS A and WAHLBORN S,
(To be published in Nuclear Physics.)

9. MONSONEGO G and PIEPENBRING R,
Excitations octupolaires et probabilités de transition E1 ($\Delta K = 0$) dans les noyaux de masse impaire de la région des terres-rares.
Nuclear Physics 78 (1966) 265.

10. FAESSLER A, UDAGAWA T and SHELINE R K,
The E1 $\Delta K = 0$ transitions in deformed odd-mass nuclei.
Nuclear Physics 85 (1966) 670.

11. GERHOLM T R and LINDSKOG J,
A magnetic coincidence spectrometer for the measurement of short nuclear lifetimes.
Arkiv Fysik 24 (1963) 171.

12. SPARRMAN P, LINDSKOG J and MARELIUS A,
An electron scintillation detector with good energy resolution.
Nuclear Instr. and Methods 41 (1966) 299.

13. GRAHAM R L, GEIGER J S, BELL R E and BARTON R,
A simple and accurate method for calibrating nanosecond time-to-pulse-height converters.
Nuclear Instr. and Methods 15 (1962) 40.

14. MALMSKOG S G,
Absolute E1 transition probabilities in the deformed nuclei Yb^{177} and Hf^{179}.
Nuclear Physics 62 (1965) 37.

15. SCHMID L C and BURSON S B,
Decay of $_{60}Nd^{151}$ (12 min).
Phys. Rev. 115 (1959) 178.

16. BLINOWSKA K J, HANSEN P G, NIELSEN H L and WILSKY K,
(Private communication.)

17. SUNDSTRÖM T,
Note on moment analysis of delayed coincidence experiments.
Nuclear Instr. and Methods 16 (1962) 153.

18. FOSSAN D B, CHASE Jr. L F and COOP K L,
Gamma rates and intensities: ℓ-forbidden M1 transitions.
Phys. Rev. 140 (1965) B1.

19. CABEZAS A Y, LINDGREN I and MARRUS R,
Atomic-beam investigations of electronic and nuclear ground states in the rare-earth region.
Phys. Rev. 122 (1961) 1796.

20. NILSSON S G, GUSTAFSON C, LAMM I L and NILSSON B,
(Private communication.)

21. BUDICK B and MARRUS R,
Hyperfine structure and nuclear moments of promethium-147 and promethium-151.
Phys. Rev. 132 (1963) 723.

22. NATHAN O and NILSSON S G,
In Alpha-, beta- and gamma-ray spectroscopy. Ed. by K Siegbahn, North Holland Publ. Co., Amsterdam, 1965.

23. Nuclear Data Sheets, Washington D.C. Dec 1964.

24. FUNKE L, GRABER H, KAUN K-H, SODAN H and FRÁNA J,
Energieniveaus und Rotations-Teilchen-Kopplung im ^{155}Eu.
Nuclear Physics 88 (1966) 641.

25. BELL R E, GRAHAM R L and PETCH H E,
Design and use of a coincidence circuit of short resolving time.
Can. J. Phys. Sect. A 30 (1952) 35.

26. LINDSKOG J and SUNDSTRÖM T,
Improved experimental methods for measurements of nuclear lifetimes down to 10^{-11} seconds.
Arkiv Fysik 24 (1963) 199.

27. MALMSKOG S G,
Hindered E1 transition in Eu^{155} and Tb^{161}.
Nuclear Physics 68 (1965) 517.

28. SLIV L A and BAND I M,
Appendix 5 in Alpha-, beta- and gamma-ray spectroscopy.
Ed. by K Siegbahn, North Holland Publ. Co., Amsterdam, 1965.

29. DE BOER J and ROGERS J D,
Concerning the magnetic properties of deformed nuclei in the region $153 \leq A \leq 187$.
Phys. Letters 3 (1963) 304.

30. VERGNES M and JASTRZEBSKI J,
Périodes des niveaux excités de $^{155}_{63}Eu$.
J. Phys. Radium 22 (1961) 669.

31. WAHLBORN S,
Variational approach to the nuclear pairing-correlation problem.
Arkiv Fysik 31 (1965) 33.

32. BROCKMEIER R T, WAHLBORN S, SEPPI E J and BOEHM F,
Coriolis coupling between rotational bands in the nucleus ^{183}W.
Nuclear Physics 63 (1965) 102.

33. WAHLBORN S,
The nuclear pairing-correlation model. 2.
Arkiv Fysik 31 (1966) 319.

34. SOLOVIEV V G and VOGEL P,
Structure of the ground and excited states of odd-mass deformed nuclei in the region $153 \leq A \leq 187$.
Nuclear Physics A92 (1967) 449.

35. METZGER F R,
Lifetimes of 1^- states in Sm^{148} and Sm^{152}.
Phys. Rev. 137 (1965) B 1415.

36. MOTTELSON B R and NILSSON S G,
The intrinsic states of odd-A nuclei having ellipsoidal equilibrium shape.
Mat.-Fys. Skr. Danske Vid. Selsk. 1 (1959) no 8.

37. HAMILTON B R and DAVIES K E,
The mean life and nuclear deformation of the 98 keV level in ^{153}Eu.
Nuclear Physics 58 (1964) 407.

38. ATZMONY U and OFER S,
Mössbauer-Effect Studies of the 97-keV level of ^{153}Eu.
Phys. Rev. 145 (1966) 915.

39. MEILING W and STARY F,
Messung von Nanosekunden - Lebensdauern an Niveaus deformierter Kerne.
Nuclear Physics 74 (1965) 113.

40. MALMSKOG S G,
(To be published.)

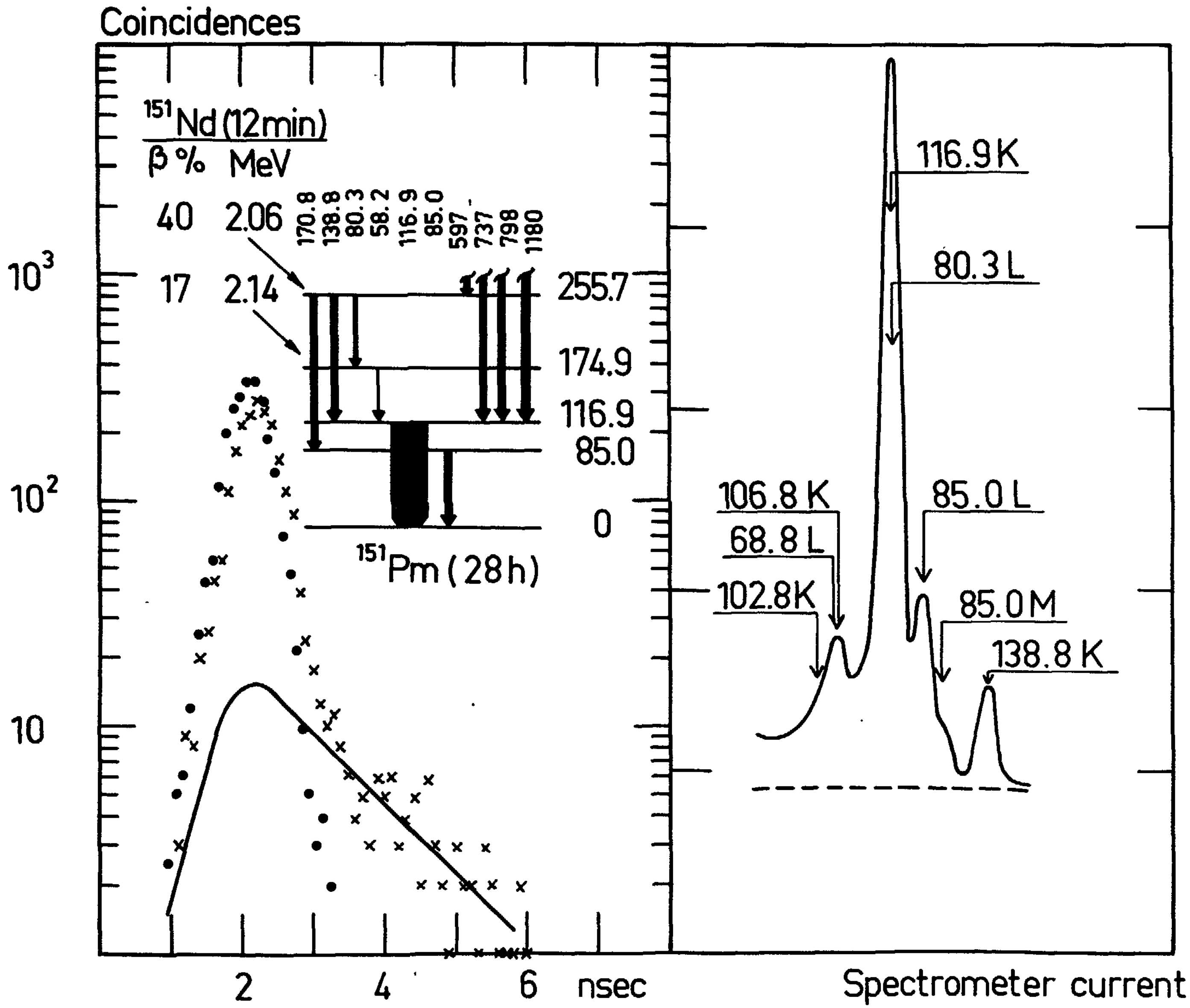
Coincidences
151Nd (12min)
β % MeV
40 2.06
17 2.14
170.8
138.8
80.3
58.2
116.9
85.0
597
737
798
1180
255.7
174.9
116.9
85.0
0
151Pm (28h)
10³
10²
10
2
4
6
nsec
116.9 K
80.3 L
106.8 K
68.8 L
102.8K
85.0 L
85.0 M
138.8 K
Spectrometer current

Fig. 1

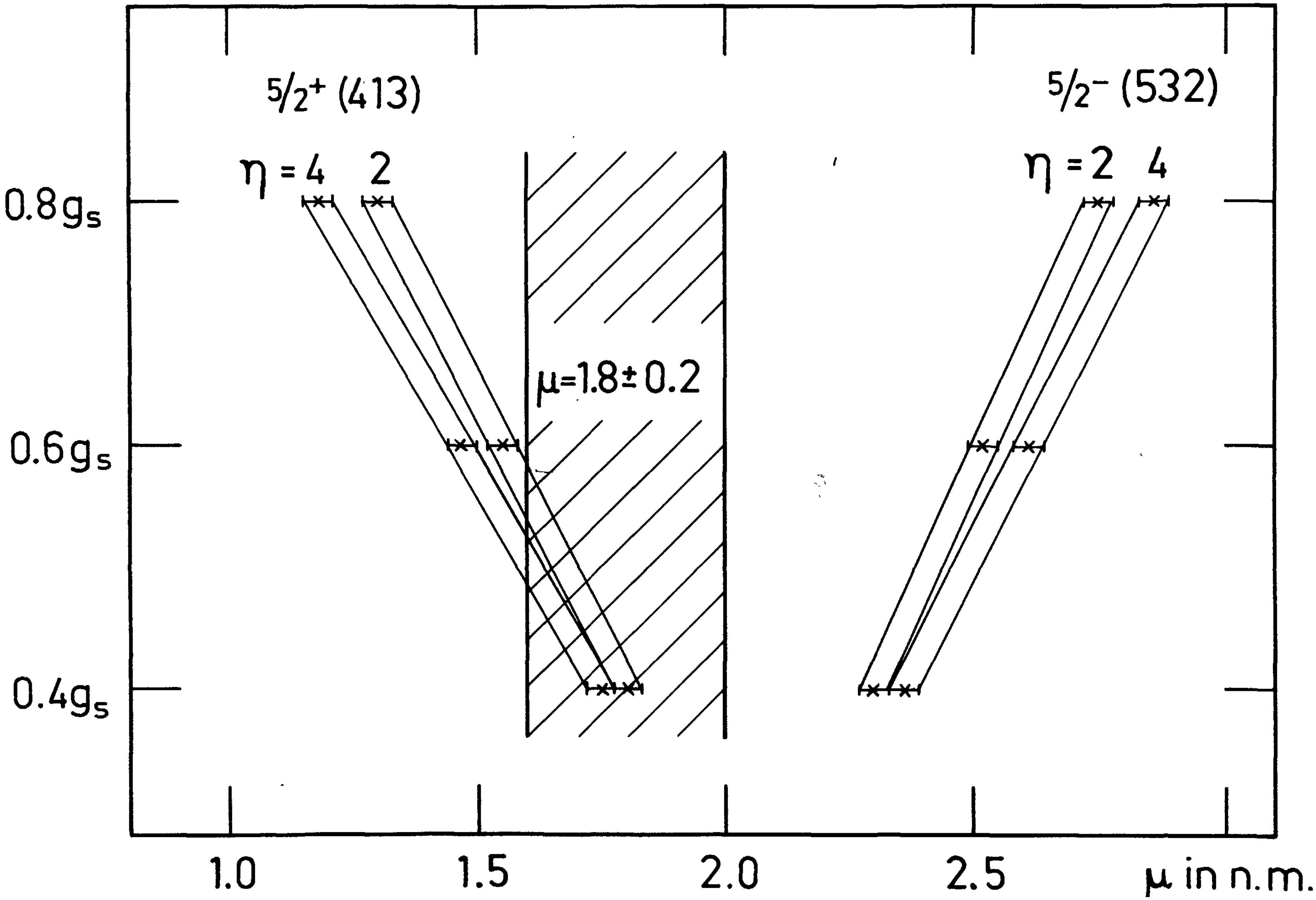

Fig. 2

Fig. 3

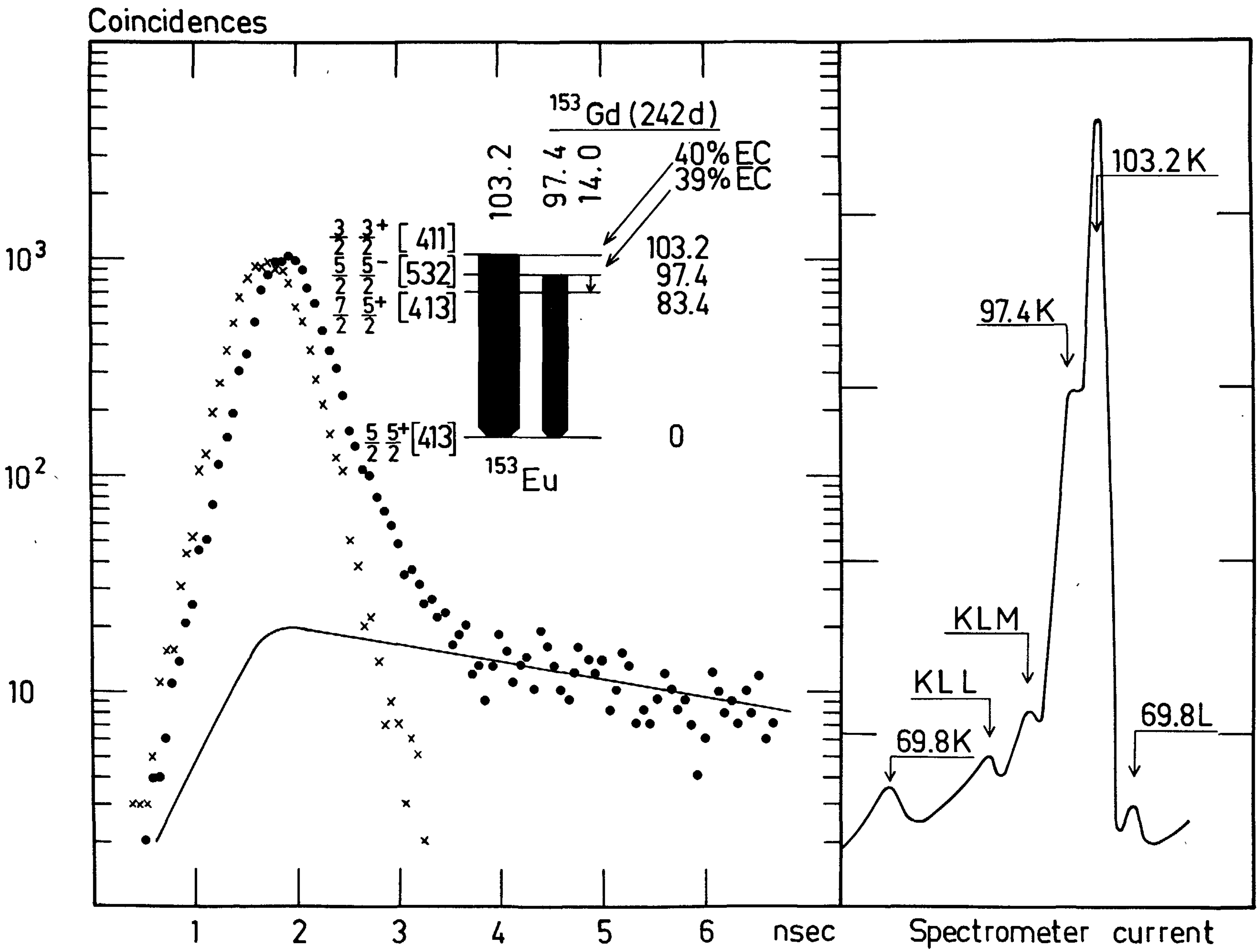

Coincidences
10^3
10^2
10
1
2
3
4
5
6
nsec
153Gd (242d)
103.2
97.4
14.0
40% EC
39% EC
3/2 3/2+ [411]
5/2 5/2− [532]
7/2 5/2+ [413]
5/2 5/2+ [413]
103.2
97.4
83.4
0
153Eu
103.2 K
97.4 K
KLM
KLL
69.8 K
69.8 L
Spectrometer current

Fig. 4

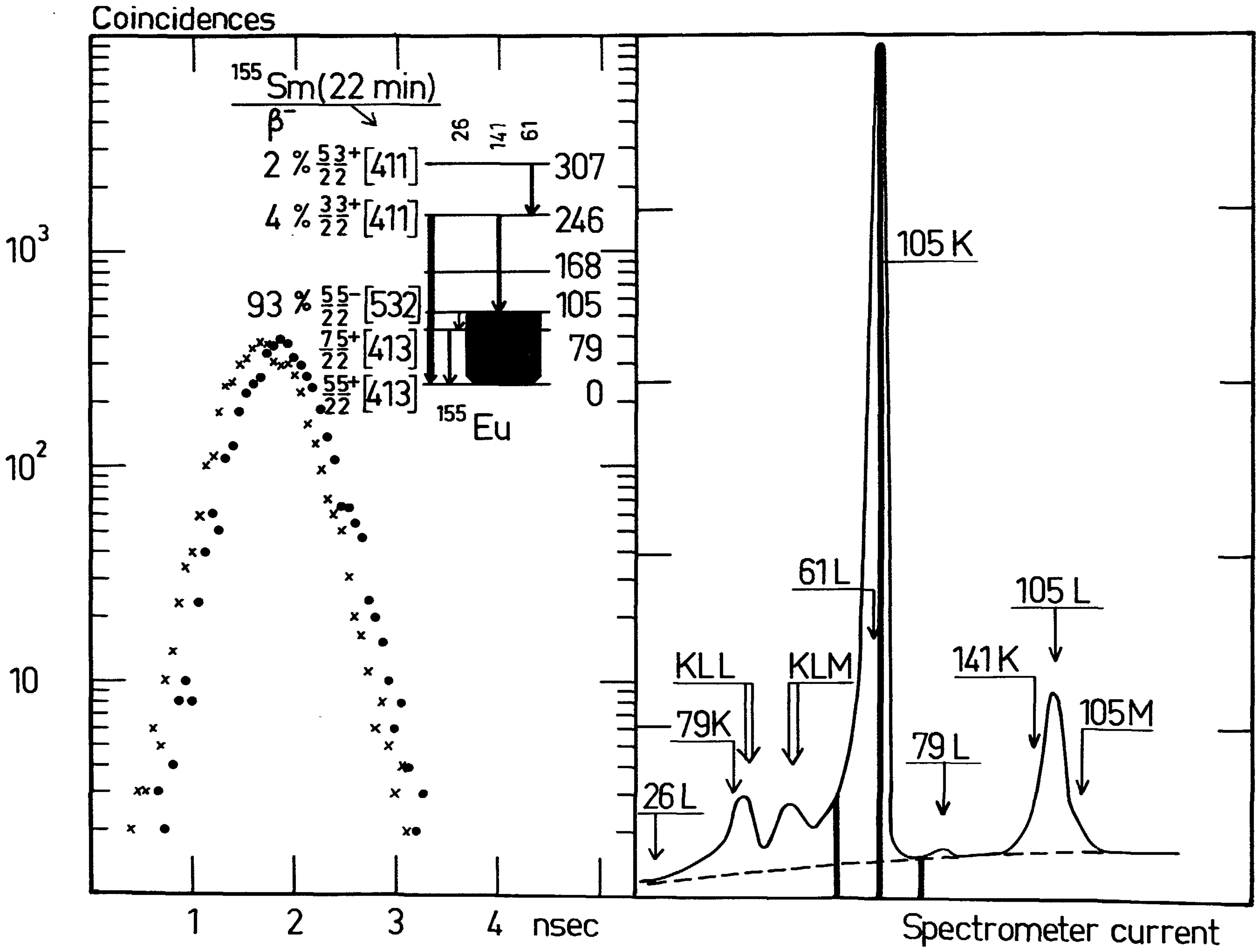

Coincidences
155 Sm(22 min)
β⁻
26
141
61
2 % 5/2 3/2+ [411]
307
4 % 3/2 3/2+ [411]
246
168
93 % 5/2 5/2− [532]
105
7/2 5/2+ [413]
79
5/2 5/2+ [413]
0
155 Eu
10³
10²
10
1
2
3
4
nsec
105 K
61 L
105 L
KLL
KLM
141 K
79K
105M
79 L
26 L
Spectrometer current

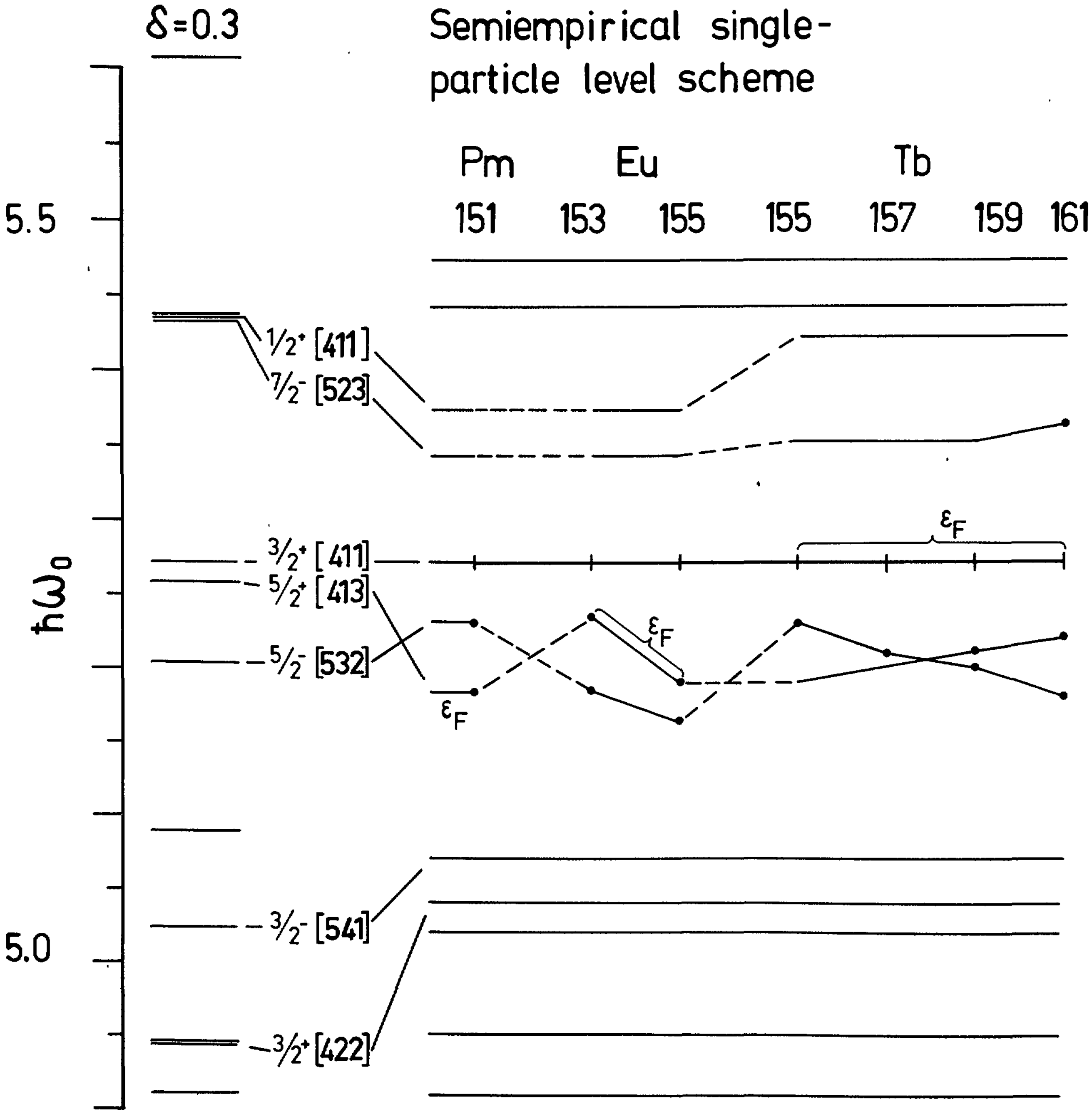
δ=0.3
Semiempirical single-particle level scheme
Pm
Eu
Tb
151
153
155
155
157
159
161
5.5
5.0
ħω₀
1/2⁺ [411]
7/2⁻ [523]
3/2⁺ [411]
5/2⁺ [413]
5/2⁻ [532]
3/2⁻ [541]
3/2⁺ [422]
ε_F
ε_F
ε_F

Fig. 5

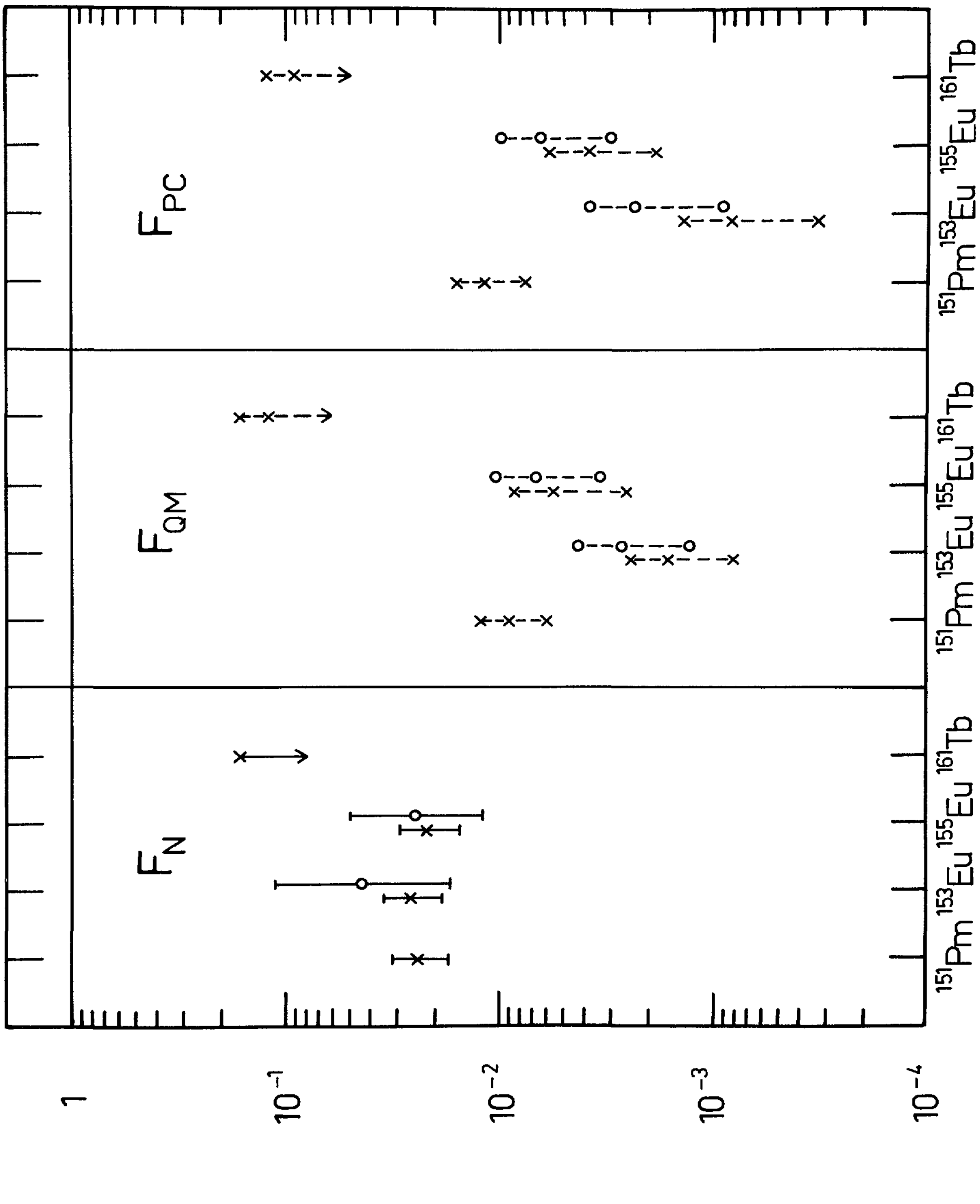

Fig. 6

LIST OF PUBLISHED AE-REPORTS

1–200. (See the back cover earlier reports.)

201. Heat transfer analogies. By A. Bhattacharyya. 1965. 55 p. Sw. cr. 8:–.
202. A study of the "384" KeV complex gamma emission from plutonium-239. By R. S. Forsyth and N. Ronqvist. 1965. 14 p. Sw. cr. 8:–.
203. A scintillometer assembly for geological survey. By E. Dissing and O. Landström. 1965. 16 p. Sw. cr. 8:–.
204. Neutron-activation analysis of natural water applied to hydrogeology. By O. Landström and C. G. Wenner. 1965. 28 p. Sw. cr. 8:–.
205. Systematics of absolute gamma ray transition probabilities in deformed odd-A nuclei. By S. G. Malmskog. 1965. 60 p. Sw. cr. 8:–.
206. Radiation induced removal of stacking faults in quenched aluminium. By U. Bergenlid. 1965. 11 p. Sw. cr. 8:–.
207. Experimental studies on assemblies 1 and 2 of the fast reactor FR0. Part 2. By E. Hellstrand, T. Andersson, B. Brunfelter, J. Kockum, S-O. Londen and L. I. Tirén. 1965. 50 p. Sw. cr. 8:–.
208. Measurement of the neutron slowing-down time distribution at 1.46 eV and its space dependence in water. By E. Möller. 1965. 29 p. Sw. cr. 8:–.
209. Incompressible steady flow with tensor conductivity leaving a transverse magnetic field. By E. A. Witalis. 1965. 17 p. Sw. cr. 8:–.
210. Methods for the determination of currents and fields in steady two-dimensional MHD flow with tensor conductivity. By E. A. Witalis. 1965. 13 p. Sw. cr. 8:–.
211. Report on the personnel dosimetry at AB Atomenergi during 1964. By K. A. Edvardsson. 1966. 15 p. Sw. cr. 8:–.
212. Central reactivity measurements on assemblies 1 and 3 of the fast reactor FR0. By S-O. Londen. 1966. 58 p. Sw. cr. 8:–.
213. Low temperature irradiation applied to neutron activation analysis of mercury in human whole blood. By D. Brune. 1966. 7 p. Sw. cr. 8:–.
214. Characteristics of linear MHD generators with one or a few loads. By E. A. Witalis. 1966. 16 p. Sw. cr. 8:–.
215. An automated anion-exchange method for the selective sorption of five groups of trace elements in neutron-irradiated biological material. By K. Samsahl. 1966. 14 p. Sw. cr. 8:–.
216. Measurement of the time dependence of neutron slowing-down and thermalization in heavy water. By E. Möller. 1966. 34 p. Sw. cr. 8:–.
217. Electrodeposition of actinide and lanthanide elements. By N-E. Bärring. 1966. 21 p. Sw. cr. 8:–.
218. Measurement of the electrical conductivity of He^3 plasma induced by neutron irradiation. By J. Braun and K. Nygaard. 1966. 37 p. Sw. cr. 8:–.
219. Phytoplankton from Lake Magelungen, Central Sweden 1960–1963. By T. Willén. 1966. 44 p. Sw. cr. 8:–.
220. Measured and predicted neutron flux distributions in a material surrounding av cylindrical duct. By J. Nilsson and R. Sandlin. 1966. 37 p. Sw. cr. 8:–.
221. Swedish work on brittle-fracture problems in nuclear reactor pressure vessels. By M. Grounes. 1966 34 p. Sw. cr. 8:–.
222. Total cross-sections of U, UO_2 and ThO_2 for thermal and subthermal neutrons. By S. F. Beshai. 1966. 14 p. Sw. cr. 8:–.
223. Neutron scattering in hydrogenous moderators, studied by the time dependent reaction rate method. By L. G. Larsson, E, Möller and S. N. Purohit. 1966. 26 p. Sw. cr. 8:–.
224. Calcium and strontium in Swedish waters and fish, and accumulation of strontium-90. By P-O. Agnedal. 1966. 34 p. Sw cr. 8:–.
225. The radioactive waste management at Studsvik. By R. Hedlund and A. Lindskog. 1966. 14 p. Sw cr. 8:–
226. Theoretical time dependent thermal neutron spectra and reaction rates in H_2O and D_2O. S. N. Purohit. 1966. 62 p. Sw. cr. 8:–.
227. Integral transport theory in one-dimensional geometries. By I. Carlvik. 1966. 65 p. Sw. cr. 8:–.
228. Integral parameters of the generalized frequency spectra of moderators By S. N. Purohit. 1966. 27 p. Sw. cr. 8:–.
229. Reaction rate distributions and ratios in FR0 assemblies 1, 2 and 3. By T. L. Andersson. 1966. 50 p. Sw. cr. 8:–.
230. Different activation techniques for the study of epithermal spectra, applied to heavy water lattices of varying fuel-to-moderator ratio. By E. K Sokolowski. 1966. 34 p. Sw. cr. 8:–.
231. Calibration of the failed-fuel-element detection systems in the Ågesta reactor. By O. Strindehag. 1966. 52 p. Sw. cr. 8:–.
232. Progress report 1965. Nuclear chemistry. Ed. by G. Carleson. 1966. 26 p Sw. cr. 8:–.
233. A summary report on assembly 3 of FR0. By T. L. Andersson, B. Brunfelter, P. F. Cecchi, E. Hellstrand, J. Kockum, S-O. Londen and L. I. Tirén. 1966. 34 p. Sw. cr. 8:–.
234. Recipient capacity of Tvären, a Baltic Bay. By P.-O. Agnedal and S. O. W. Bergström. 1966. 21 p. Sw. cr. 8:–.
235. Optimal linear filters for pulse height measurements in the presence of noise. By K. Nygaard. 1966. 16 p. Sw. cr. 8:–.
236. DETEC, a subprogram for simulation of the fast-neutron detection process in a hydro-carbonous plastic scintillator. By B. Gustafsson and O. Aspelund. 1966. 26 p. Sw. cr. 8:–.
237. Microanalys of fluorine contamination and its depth distribution in zircaloy by the use of a charged particle nuclear reaction. By E. Möller and N Starfelt. 1966. 15 p. Sw. cr. 8:–.
238. Void measurements in the regions of sub-cooled and low-quality boiling. P. 1. By S. Z. Rouhani. 1966. 47 p. Sw. cr. 8:–.
239. Void measurements in the regions of sub-cooled and low-quality boiling. P. 2. By S. Z. Rouhani. 1966. 60 p. Sw. cr. 8:–.
240. Possible odd parity in ^{128}Xe. By L. Broman and S. G. Malmskog. 1966. 10 p. Sw. cr. 8:–.
241. Burn-up determination by high resolution gamma spectrometry: spectra from slightly-irradiated uranium and plutonium between 400–830 keV. By R. S. Forsyth and N. Ronqvist. 1966. 22 p. Sw. cr. 8:–.
242. Half life measurements in ^{155}Gd. By S. G. Malmskog. 1966. 10 p. Sw. cr. 8:–.
243. On shear stress distributions for flow in smooth or partially rough annuli. By B. Kjellström and S. Hedberg. 1966. 66 p. Sw. cr. 8:–.
244. Physics experiments at the Ågesta power station. By G. Apelqvist, P.-Å. Bliselius, P. E. Blomberg, E. Jonsson and F. Åkerhielm. 1966. 30 p. Sw. cr. 8:–.
245. Intercrystalline stress corrosion cracking of inconel 600 inspection tubes in the Ågesta reactor. By B. Grönwall, L. Ljungberg, W. Hübner and W. Stuart. 1966. 26 p. Sw. cr. 8:–.
246. Operating experience at the Ågesta nuclear power station. By S. Sandström. 1966. 113 p. Sw. cr. 8:–.
247. Neutron-activation analysis of biological material with high radiation levels By K. Samsahl. 1966. 15 p. Sw. cr. 8:–.
248. One-group perturbation theory applied to measurements with void. By R Persson. 1966. 19 p. Sw. cr. 8:–.
249. Optimal linear filters. 2. Pulse time measurements in the presence of noise. By K. Nygaard. 1966 9 p. Sw. cr. 8:–.
250. The interaction between control rods as estimated by second-order one-group perturbation theory. By R. Persson. 1966. 42 p. Sw. cr. 8:–.
251. Absolute transition probabilities from the 453.1 keV level in 183W. By S. G Malmskog. 1966. 12 p. Sw. cr. 8:–.
252. Nomogram for determining shield thickness for point and line sources of gamma rays. By C. Jönemalm and K. Malén. 1966. 33 p. Sw. cr. 8:–
253. Report on the personnel dosimetry at AB Atomenergi during 1965. By K. A Edwardsson. 1966. 13 p. Sw. cr. 8:–.
254 Buckling measurements up to 250°C on lattices of Ågesta clusters and on D_2O alone in the pressurized exponential assembly TZ. By R. Persson. A. J. W. Andersson and C.-E. Wikdahl. 1966. 56 p. Sw. cr. 8:–.
255. Decontamination experiments on intact pig skin contaminated with beta-gamma-emitting nuclides. By K. A. Edwardsson, S. Hagsgård and Å. Swensson. 1966. 35 p. Sw. cr. 8:–.
256. Pertubation method of analysis applied to substitution measurements of buckling. By R. Persson. 1966. 57 p. Sw. cr. 8:–.
257. The Dancoff correction in square and hexagonal lattices. By I. Carlvik. 1966 35 p. Sw. cr. 8:–.
258. Hall effect influence on a highly conducting fluid. By E. A. Witalis. 1966 13 p. Sw. cr. 8:–.
259. Analysis of the quasi-elastic scattering of neutrons in hydrogenous liquids By S. N. Purohit. 1966. 26 p. Sw. cr. 8:–.
260. High temperature tensile properties of unirradiated and neutron irradiated 20Cr–35Ni austenitic steel By R B Roy and B Solly. 1966. 25 p. Sw cr. 8:–.
261. On the attenuation of neutrons and photons in a duct filled with a helical plug. By E. Aalto and Å. Krell 1966. 24 p. Sw. cr 8:–.
262. Design and analysis of the power control system of the fast zero energy reactor FR-O. By N. J. H. Schuch. 1966. 70 p. Sw. cr 8:–.
263. Possible deformed states in ^{115}In and ^{117}In. By A. Bäcklin, B. Fogelberg and S. G. Malmskog. 1967. 39 p. Sw. cr. 10:–.
264. Decay of the 16.3 min. ^{182}Ta isomer. By M. Höjeberg and S. G. Malmskog 1967. 13 p. Sw. cr. 10:–.
265. Decay properties of ^{147}Nd. By A. Bäcklin and S. G. Malmskog. 1967. 15 p. Sw. cr. 10: –.
266. The half life of the 53 keV level in ^{197}Pt. By S. G. Malmskog. 1967. 10 p. Sw. cr. 10:–.
267. Burn-up determination by hight resolution gamma spectrometry: Axial and diametral scanning experiments. By R. S. Forsyth, W. H. Blackadder and N. Ronqvist. 1967. 18 p. Sw. cr. 10:–.
268. On the properties of the $s_{1/2} \longrightarrow d_{3/2}$ transition in ^{199}Au. By A. Bäcklin and S. G. Malmskog. 1967. 23 p. Sw. cr. 10:–.
269. Experimental equipment for physics studies in the Ågesta reactor. By G. Bernander, P. E. Blomberg and P.-O. Dubois. 1967. 35 p. Sw. cr. 10:–.
270. An optical model study of neutrons elastically scattered by iron, nickel, cobalt, copper, and indium in the energy region 1.5 to 7.0 MeV. By B. Holmqvist and T. Wiedling. 1967. 20 p. Sw. cr. 10:–.
271. Improvement of reactor fuel element heat transfer by surface roughness. By B. Kjellström and A. E. Larsson. 1967. 94 p. Sw. cr. 10:–.
272. Burn-up determination by high resolution gamma spectrometry Fission product migration studies. By R. S. Forsyth, W. H. Blackadder and N. Ronqvist. 1967. 19 p. Sw. cr. 10:–.
273. Monoenergetic critical parameters and decay constants for small spheres and thin slabs. By I. Carlvik. 24 p. Sw. cr. 10:–.
274. Scattering of neutrons by an anharmonic crystal. By T. Högberg, L. Bohlin and I. Ebbsjö. 1967. 38 p. Sw. cr. 10:–.
275. The $I\Delta KI=1$, E1 transitions in odd-A isotopes of Tb and Eu. By S. G. Malmskog, A. Marelius and S. Wahlborn. 1967. 24 p. Sw. cr. 10:–.
276. A burnout correlation for flow of boiling water in vertical rod bundles. By Kurt M. Becker. 1967. 102 p. Sw. cr. 10:–.
277. Epithermal and thermal spectrum indices in heavy water lattices. By E. K. Sokolowski and A. Jonsson. 1967. 44 p. Sw. cr. 10:–.
278. On the $d_{5\,2} \leftrightarrow g_{7/2}$ transitions in odd mass Pm nuclei. By A. Bäcklin and S. G. Malmskog. 1967. 14 p. Sw. cr. 10:–.
279. Calculations of neutron flux distributions by means of integral transport methods. By I. Carlvik. 1967. 94 p. Sw. cr. 10:–.
280. On the magnetic properties of the K=1 rotational band in ^{188}Re. By S. G. Malmskog and M. Höjeberg. 1967. 18 p. Sw. cr. 10:–.
281. Collision probabilities for finite cylinders and cuboids. By I. Carlvik. 1967. 28 p. Sw. cr. 10:–.
282. Polarized elastic fast-neutron scattering off ^{12}C in the lower MeV-range. I. Experimental part. By O. Aspelund. 1967. 50 p. Sw. cr. 10:–.
283. Progress report 1966 nuclear chemistry. 1967. 26 p. Sw. cr. 10:–.
284. Finite-geometry and polarized multiple-scattering corrections of experimental fast-neutron polarization data by means of Monte Carlo methods. By O. Aspelund and B. Gustafsson. 1967. 60 p. Sw. cr. 10:–.
285. Power disturbances close to hydrodynamic instability in natural circulation two-phase flow. By R. P. Mathisen and O. Eklind. 1967. 34 p. Sw. cr. 10:–.
286. Calculation of steam volume fraction in subcooled boiling. 1967. 26 p. Sw. cr. 10:–.
287. Absolute E1, $\Delta K=0$ transition rates in odd-mass Pm and Eu-isotopes. By S. G. Malmskog. 1967. 33 p. Sw cr. 10: –.

Förteckning över publicerade AES-rapporter

1. Analys medelst gamma-spektrometri. Av D. Brune. 1961. 10 s Kr 6:–.
2. Bestrålningsförändringar och neutronatmosfär i reaktortrycktankar – några synpunkter. Av M. Grounes. 1962. 33 s. Kr 6:–.
3. Studium av sträckgränsen i mjukt stål. Av G. Östberg och R. Attermo 1963. 17 s. Kr 6:–.
4. Teknisk upphandling inom reaktorområdet. Av Erik Jonson. 1963. 64 s Kr 8:–.
5. Ågesta Kraftvärmeverk. Sammanställning av tekniska data, beskrivningar m. m. för reaktordelen. Av B. Lilliehöök. 1964. 336 s. Kr 15:–.
6. Atomdagen 1965. Sammanställning av föredrag och diskussioner. Av S Sandström. 1966. 321 s. Kr 15:–.

Additional copies available at the library of AB Atomenergi, Studsvik, Nyköping, Sweden. Micronegatives of the reports are obtainable through Filmprodukter, Gamla landsvägen 4, Ektorp, Sweden.

EOS-tryckerierna, Stockholm 1967